

# Perturbation theory for resonant states near a bound state in the continuum

Nan Zhang\* and Ya Yan Lu

*Department of Mathematics, City University of Hong Kong, Kowloon, Hong Kong, China*

(Dated: August 16, 2024)

In this work, we develop a perturbation theory to analyze resonant states near a bound state in the continuum (BIC) in photonic crystal slabs. The theory allows us to rigorously determine the asymptotic behavior of  $Q$ -factor and the far-field polarization. We show that the resonant states near a BIC can be nearly circularly polarized if the scattering matrix is subject to a certain condition. Moreover, our theory offers a novel perspective on super-BICs and provides a clear and precise condition to efficiently identify them in both symmetric and asymmetric structures without requiring a merging process. For practical applications, we find a super-BIC in a square lattice of finite-length cylinders on a dielectric substrate. Our theory addresses the non-Hermitian nature of the system, can be generalized to treat other structures that support BICs, and has potential applications in resonance and chiral optics.

Bound states in the continuum (BICs) are characterized by their ability to maintain localization within a continuous spectrum of radiation states [1–10]. In a photonic crystal (PhC) slab, a BIC is surrounded by resonant states with  $Q$ -factor approaching infinity [8–13]. The high- $Q$  resonances and the related strong local fields [14] can be used to enhance light-matter interactions for applications in solid-state lasing [15], sensing [16], and nonlinear optics [17], etc. Merging multiple BICs to a special BIC, which is also referred to as a super-BIC by some authors [17–30], can improve the  $Q$ -factor of nearby resonant states over a broad wavevector range and reduce the radiation losses caused by fabrication imperfections [19, 21]. In the momentum space, a BIC corresponds to a polarization singularity and is also a center of polarization vortex which has been observed experimentally [31, 32]. Such singularities can be used to manipulate light, giving rise to vortex beams generation and beam shifts [33, 34]. The far-field polarized states winding around the BIC induces a topological charge, which can intuitively describe the evolution, generation, and annihilation of BICs [35–42].

The far-field polarizations and  $Q$ -factor of resonant states near a BIC are crucial properties for understanding resonance-enhanced wave phenomena and exploring their applications. Existing studies on these two concepts are mostly numerical results, while some analytical results have been reported, they are tailored to specific models [19, 25, 43–45] or particular cases [17, 18]. In this Letter, we develop a non-Hermitian perturbation theory for resonant states near a BIC in PhC slabs. We show that if the scattering matrix satisfies a certain condition, the resonant states near the BIC can be nearly circularly polarized, which may have potential applications in areas such as chiral emission, chiroptical resonances and circular dichroism [46–50]. Moreover, our theory offers a novel perspective on super-BICs and provides a clear and precise condition to find them efficiently in symmetric and asymmetric structures without following a tedious

merging process. All existing examples of super-BICs are calculated by maintaining the up-down mirror symmetry and following a merging process [18–30]. For practical applications, the process requires heavy computation workload. Based on our theory, we find a super-BIC in a square lattice of periodic cylinders on a dielectric substrate. To the best of our knowledge, super-BICs in a biperiodic structure with broken up-down mirror symmetry have never been reported before.

To simplify the presentation, we consider a PhC slab and study resonant states with a single radiation channel near a non-degenerate BIC. The slab has a period  $L$  in both  $x$  and  $y$  and is sandwiched between two homogeneous media with dielectric constants  $\varepsilon^\pm$ , where the symbols “ $\pm$ ” indicate above and below the slab, respectively. We emphasize that our theory can accommodate more complicated scenarios, such as arbitrary periodic directions, multiple radiation channels, and even degenerate cases [50–53]. The electric field of a resonant state can be written as  $\mathbf{E} = \mathbf{u}(\boldsymbol{\rho}, z)e^{i\boldsymbol{\alpha}\cdot\boldsymbol{\rho}}$ , where  $\boldsymbol{\rho} = (x, y)$ ,  $\boldsymbol{\alpha} = (\alpha, \beta)$  is the Bloch wavevector,  $\mathbf{u}$  is periodic in  $\boldsymbol{\rho}$  and satisfies the wave equation

$$\mathcal{L}\mathbf{u} := (\nabla + i\boldsymbol{\alpha}) \times (\nabla + i\boldsymbol{\alpha}) \times \mathbf{u} = \frac{\omega^2}{c^2}\varepsilon(\boldsymbol{\rho}, z)\mathbf{u}. \quad (1)$$

The far-field polarization vector of the resonant state in  $sp$  plane is given by  $\mathbf{d}^\pm = d_s^\pm \hat{s} + d_p^\pm \hat{p}^\pm$ .

We use subscript “\*” to denote the qualities of a BIC. In addition, we normalize the BIC by  $\langle \mathbf{u}_* | \varepsilon | \mathbf{u}_* \rangle = 1$ . When the resonant state is close to the BIC, we can write  $\boldsymbol{\alpha}$  as  $\boldsymbol{\alpha}_* + \delta\hat{\nu}/L$ , where  $\delta$  is a small positive parameter and  $\hat{\nu} = (\cos\theta, \sin\theta)$ ,  $-\pi \leq \theta < \pi$  is a unit vector. If  $\delta$  is sufficiently small, the frequency  $\omega$ , the periodic state  $\mathbf{u}$  and the operator  $\mathcal{L}$  can be expanded by

$$\omega = \omega_* + \delta\omega_1(\theta) + \delta^2\omega_2(\theta) + \dots \quad (2)$$

$$\mathbf{u} = \mathbf{u}_* + \delta\mathbf{u}_1(\theta) + \delta^2\mathbf{u}_2(\theta) + \dots \quad (3)$$

$$\mathcal{L} = \mathcal{L}_* + \delta\mathcal{L}_1(\theta) + \delta^2\mathcal{L}_2(\theta), \quad (4)$$

where  $\mathcal{L}_1$  and  $\mathcal{L}_2$  are operators depending on the angle  $\theta$  and can be written down explicitly.

\* nzhang234-c@my.cityu.edu.hk

Substituting Eqs. (2)-(4) into Eq. (1) and collecting terms with the same order, we obtain a sequence of recursive equations. As shown in Supplementary Material, for each  $\theta$ , the far-field pattern of the 1st-order state correction  $\mathbf{u}_1$  is exactly a plane wave with the polarization vector  $\mathbf{d}_1^\pm = d_{1s}^\pm \hat{s}_* + d_{1p}^\pm \hat{p}_*$ . Moreover, the second-order radiation loss of resonant states near the BIC depends on the outgoing power of the plane wave, i.e.,

$$2\omega_* \text{Im}(\omega_2)L = -c^2 (\gamma_*^+ |d_1^+|^2 + \gamma_*^- |d_1^-|^2), \quad (5)$$

where  $\gamma_*^\pm = \sqrt{\omega_*^2 \varepsilon^\pm / c^2 - |\boldsymbol{\alpha}_*|^2}$ .

The polarization vector  $\mathbf{d}_1^\pm$  can be determined by involving the radiation states (diffraction solutions) corresponding to the BIC. When the slab is illuminated by  $s$  and  $p$  polarized incident plane waves in the upper and lower regions, we obtain four linearly independent radiation states  $\mathbf{u}_{s*}^\pm$  and  $\mathbf{u}_{p*}^\pm$ . If the radiation states and the BIC are orthogonal, i.e.,  $\langle \mathbf{u}_{l*}^\pm | \varepsilon | \mathbf{u}_* \rangle = 0$ ,  $l \in \{s, p\}$ , we obtain the following formula for  $\mathbf{d}_1^\pm$

$$\begin{bmatrix} d_{1s}^+ \\ d_{1p}^+ \\ d_{1s}^- \\ d_{1p}^- \end{bmatrix} = \boldsymbol{\Gamma}^{-1/2} \mathbf{S} \mathbf{U} \begin{bmatrix} \cos \theta \\ \sin \theta \end{bmatrix}, \quad (6)$$

where  $\boldsymbol{\Gamma} = \text{diag}(\gamma_*^+, \gamma_*^+, \gamma_*^-, \gamma_*^-)L$ ,  $\mathbf{S}$  is the scattering matrix, and  $\mathbf{U}$  is a  $4 \times 2$  matrix given by

$$\mathbf{U} = \begin{bmatrix} \mathbf{U}^+ \\ \mathbf{U}^- \end{bmatrix}, \quad \mathbf{U}^\pm = \begin{bmatrix} U_{sx}^\pm & U_{sy}^\pm \\ U_{px}^\pm & U_{py}^\pm \end{bmatrix}.$$

Here  $U_{l\sigma}^\pm = L^2 \langle \mathbf{u}_{l*}^\pm | \mathcal{L}_{1\sigma} | \mathbf{u}_* \rangle$  for  $l \in \{s, p\}$  and  $\sigma \in \{x, y\}$ . The operators  $\mathcal{L}_{1\sigma}$  are defined from the decomposition  $\mathcal{L}_1(\theta) = \mathcal{L}_{1x} \cos \theta + \mathcal{L}_{1y} \sin \theta$ . The detailed derivation of Eq. (6) is given in Supplementary Material (see Sec. S1).

From Eqs. (2)-(6), it is evident that if  $\mathbf{d}_1^\pm \neq 0$ , we have  $Q \sim 1/\delta^2$  and  $\mathbf{d}^\pm \sim \delta \mathbf{d}_1^\pm$  as  $\delta \rightarrow 0$ . If  $\mathbf{d}_1^\pm = 0$ , the asymptotic behavior of the  $Q$ -factor and the polarization depends on higher order state corrections. In that case, we have  $Q \sim 1/\delta^4$  at least and the BIC is a super-BIC. Consequently, our theory offers a new perspective on super-BICs, namely, the ultrahigh- $Q$  resonances are caused by a nonradiating 1st-order state correction. Notice that the above analysis does not rely on any in-plane symmetry of the structure and the theory is general.

Many theoretical studies and applications favor structures with an in-plane inversion symmetry, since then BICs can exist robustly [35]. In the following, we incorporate that symmetry into the analysis. We consider a PhC slab with an inversion symmetry, and scale the BIC such that  $\mathcal{C}_2 \bar{\mathbf{u}}_* = -\mathbf{u}_*$ , where  $\mathcal{C}_2$  is a  $180^\circ$  rotation operator around the  $z$  axis [35, 54]. We show that the matrix  $\mathbf{V} = \mathbf{S}^{1/2} \mathbf{U}$  is real, and if  $\mathbf{V}$  is full rank, then  $\mathbf{d}_1^\pm \neq 0$  for all  $\theta$  (see Sec. S2 in Supplementary Material). We refer to such a BIC as a generic BIC. A super-BIC has a vanishing  $\mathbf{d}_1^\pm$  at all or some angles, corresponding to a rank-deficient  $\mathbf{V}$ . More precisely, super-BICs can be categorized into two classes:

*class 1:*  $\mathbf{V} = 0$ . We have  $\mathbf{d}_1^\pm = 0$  and  $Q \sim 1/\delta^4$  at least for all  $\theta$ . The ultrahigh- $Q$  resonances occur in all directions.

*class 2:*  $\text{rank}(\mathbf{V}) = 1$ . We only have an angle  $0 \leq \theta_s < \pi$  such that  $[\cos \theta_s, \sin \theta_s]^\top$  belongs to the null space of  $\mathbf{V}$ . For  $\theta \neq \theta_s, \theta_s - \pi$ , we have  $\mathbf{d}_1^\pm \neq 0$  and  $Q \sim 1/\delta^2$ . For  $\theta = \theta_s, \theta_s - \pi$ , we have  $\mathbf{d}_1^\pm = 0$  and  $Q \sim 1/\delta^4$  at least. The ultrahigh- $Q$  resonances occur only in these two directions, and the asymptotic growth order of  $Q$ -factor exhibits directionality.

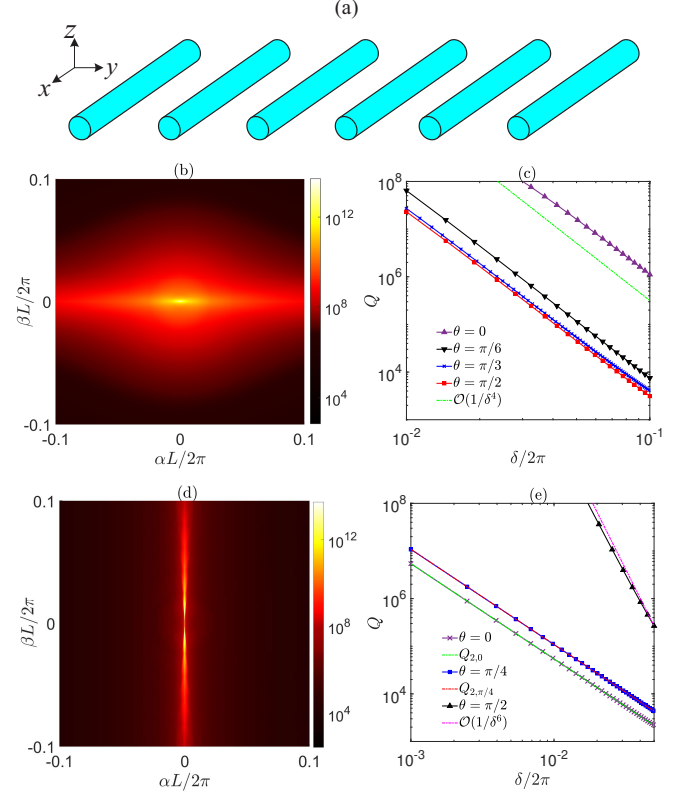


FIG. 1. (a). Schematic of a periodic array of circular cylinders. (b) and (c).  $Q$ -factor of resonant states near an at- $\Gamma$  BIC with  $\mathcal{C}_2 \mathbf{u}_* = -\mathbf{u}_*$  and asymptotic behavior of  $Q$ -factor at four angles. (d) and (e).  $Q$ -factor of resonant states near a super-BIC with  $\mathcal{C}_2 \mathbf{u}_* = \mathbf{u}_*$  and asymptotic behavior of  $Q$ -factor at three angles. The values of  $Q$  are nearly identical with the values of  $Q_{2,\theta}$  calculated by our theory.

We provide several numerical examples to verify our theory. For an at- $\Gamma$  BIC, the related radiation states can be scaled such that  $\mathcal{C}_2 \mathbf{u}_{l*}^\pm = -\mathbf{u}_{l*}^\pm$ . If the BIC is not symmetry-protected ( $\mathcal{C}_2 \mathbf{u}_* = -\mathbf{u}_*$ ), according to the anticommutativity of operators  $\mathcal{L}_{1\sigma}$  and  $\mathcal{C}_2$ , i.e.,  $\mathcal{L}_{1\sigma} \mathcal{C}_2 = -\mathcal{C}_2 \mathcal{L}_{1\sigma}$ , we have  $U_{l\sigma}^\pm = 0$  and obtain a zero  $\mathbf{V}$ . In this case, we typically have  $Q \sim 1/\delta^4$  for all  $\theta$  and this BIC is a super-BIC belonging to *class 1*. As an example, we consider a periodic array of infinitely long circular cylinders with the radius  $R$  and the dielectric constant  $\varepsilon_c$  shown in Fig. 1(a). The structure is surrounded by air. At  $R = 0.4441L$  and  $\varepsilon_c = 15$ , we obtain a BIC in a TE band with  $\mathcal{C}_2 \mathbf{u}_* = -\mathbf{u}_*$ . Figure 1(b) and (c) show that we

indeed have  $Q \sim 1/\delta^4$  for all  $\theta$ . In addition, we consider a BIC belonging to the irreducible  $B$  representation in a PhC slab with  $C_{6v}$  symmetry [35, 54]. Such a BIC also satisfies  $\mathcal{C}_2 \mathbf{u}_* = -\mathbf{u}_*$  and we then have  $Q \sim 1/\delta^4$  in all directions at least.

A symmetry-protected BIC typically is generic and has a full rank matrix  $\mathbf{V}$ . It becomes a super-BIC if the matrix  $\mathbf{V}$  is rank-deficient. As an illustration, we consider a periodic array of infinitely long circular cylinders. The matrix  $\mathbf{V}$  of a BIC in a TE band holds the form

$$\mathbf{V} = \begin{bmatrix} 0 & V_{12} \\ V_{21} & 0 \\ 0 & V_{32} \\ V_{41} & 0 \end{bmatrix}, \quad (7)$$

and we have  $V_{12} = V_{32}$  and  $V_{21} = V_{41}$  due to up-down mirror symmetry. At  $\varepsilon_c = 8.2$  and  $R = 0.4404L$ , we have a super-BIC with  $V_{12} = 0$  and  $V_{21} = 0.1696$ . From Eq. (6), we have  $\mathbf{d}_1^\pm = 0$  for  $\theta_s = \pm\pi/2$ . Moreover, since the BIC is symmetry-protected, we can further prove that  $Q \sim 1/\delta^6$  at least (see Sec. S3 in Supplementary Material). For other  $\theta$ , we can calculate the vectors  $\mathbf{d}_1^\pm$  from Eq. (6) and approximate  $Q$ -factor by  $Q_{2,\theta} = 0.5\omega_*/\text{Im}[\delta^2\omega_2(\theta)]$ . Figure 1(d) and (e) demonstrate the validity of our theory.

For at- $\Gamma$  BICs in structures with  $C_{4v}$  symmetry, the related radiation states belong to the irreducible  $E$  representation. We consider BICs belonging to the irreducible  $A_2$  representation and show that the matrix  $\mathbf{V}$  holds the form in Eq. (7) with  $V_{12} = -V_{21}$  and  $V_{32} = -V_{41}$ . A super-BIC corresponds to  $V_{12} = V_{32} = 0$ . In this case, we can further prove that  $Q \sim 1/\delta^6$  for all  $\theta$  at least (see Sec. S3 in Supplementary Material). For BICs belonging to other representations, our theory remains valid. All existing examples on super-BICs in structures with  $C_{4v}$  symmetry are obtained by searching off- $\Gamma$  BICs and following a merging process [19, 28]. Our theory provides a clear condition to find super-BICs efficiently without these time-consuming processes. In fact, we only need to tune some structural parameters to find common zeros of  $V_{12}$  and  $V_{32}$ . To validate our theory, we consider a square lattice of finite-length silicon circular cylinders ( $\varepsilon_{\text{Si}} = 12$ ) embedded in air. We have  $V_{12} = V_{32}$  due to up-down mirror symmetry and only need to tune one parameter to obtain a zero of  $V_{12}$ . We fix the height  $h$  and show the quality  $V_{12}$  as a function of radius  $R$  in Fig. 2(a). It can be seen that at  $R = 0.22105L$ , we have  $V_{12} = 0$  and obtain a super-BIC (marked by a gray hexagram). As indicated in Fig. 2(b)-(c), we indeed have  $Q \sim 1/\delta^6$ . We also show the  $Q$ -factor of resonant states near a generic BIC at  $R = 0.24L$  in Fig. 3(c) and (d). It is obvious that super-BICs can improve the  $Q$ -factor in a broad wavevector range.

If the structure breaks up-down mirror symmetry, we have  $V_{12} \neq V_{32}$  and usually need to tune two structural parameters to find common zeros of  $V_{12}$  and  $V_{32}$ . As an example, we consider a square lattice of finite-length silicon cylinders on a silica substrate ( $\varepsilon_{\text{SiO}_2} = 2.1025$ )

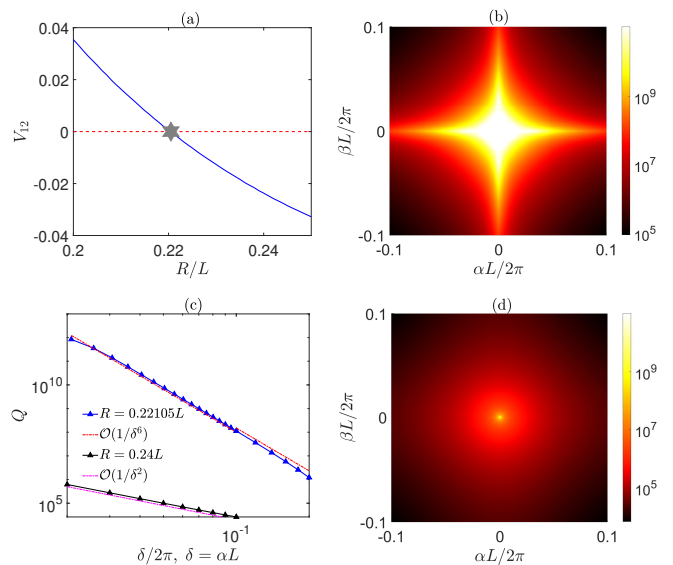


FIG. 2. (a). The quantity  $V_{12}$  as a function of radius  $R$ . (b).  $Q$ -factor of resonant states near a super-BIC at  $R = 0.22105L$ . (c). Asymptotic behavior of  $Q$ -factor. (d).  $Q$ -factor of resonant states near a generic BIC at  $R = 0.24L$ .

shown in Fig. 3(a). The qualities  $V_{12}$  and  $V_{32}$  as functions of radius  $R$  for two values of height,  $h = 0.8L$  and  $0.82045L$ , are shown in Fig. 3(b) and (c). Compared with the previous example, for the same height  $h = 0.8L$ , the curves of  $V_{12}$  and  $V_{32}$  are different and zeros of  $V_{12}$  and  $V_{32}$  also do not coincide. As the height  $h$  is increased to  $0.82045L$ , zeros of  $V_{12}$  and  $V_{32}$  coincide at  $R = 0.2362L$  and we obtain a super-BIC (marked by a blue pentagram). As shown in Fig. 3(d)-(e), we have  $Q \sim 1/\delta^6$  in all directions. The above results indicate that based on our theory, super-BICs can be efficiently identified even in the absence of up-down mirror symmetry. However, finding such a super-BIC using a merging approach is remarkably challenging, as it requires the tuning of a parameter to find off- $\Gamma$  BICs, and further tuning to merge them with an at- $\Gamma$  BIC. This process is tedious and involves cumbersome parameter adjustments.

The preceding analysis has examined the asymptotic behavior of  $Q$ -factor. In the following, we study the far-field polarization of resonant states near generic BICs. Our theory applies to super-BICs as well. For simplicity, we consider a structure with up-down mirror symmetry and drop superscript “ $\pm$ ” in  $\mathbf{d}^\pm$  and  $\mathbf{d}_1^\pm$ , where  $\mathbf{d}^\pm$  and  $\mathbf{d}_1^\pm$  are far-field polarization vectors of resonant states  $\mathbf{u}$  and 1st-order state corrections  $\mathbf{u}_1$ , respectively. The polarization angles for  $\mathbf{d}$  and  $\mathbf{d}_1$  are defined by  $\phi = \arg(S_1 + iS_2)/2$  and  $\phi_1 = \arg(S_{1,1} + iS_{1,2})/2$ , respectively, where  $S_1 = |d_s|^2 - |d_p|^2$ ,  $S_2 = 2\text{Re}(d_s \bar{d}_p)$ , and  $S_{1,1}$ ,  $S_{1,2}$  are defined in a similar manner. It is clear that  $\phi \sim \phi_1$  as  $\delta \rightarrow 0$ .

Whether there are circularly polarized states arbitrarily close to a BIC is an important theoretical question [35]. In the following, we show that there exist some

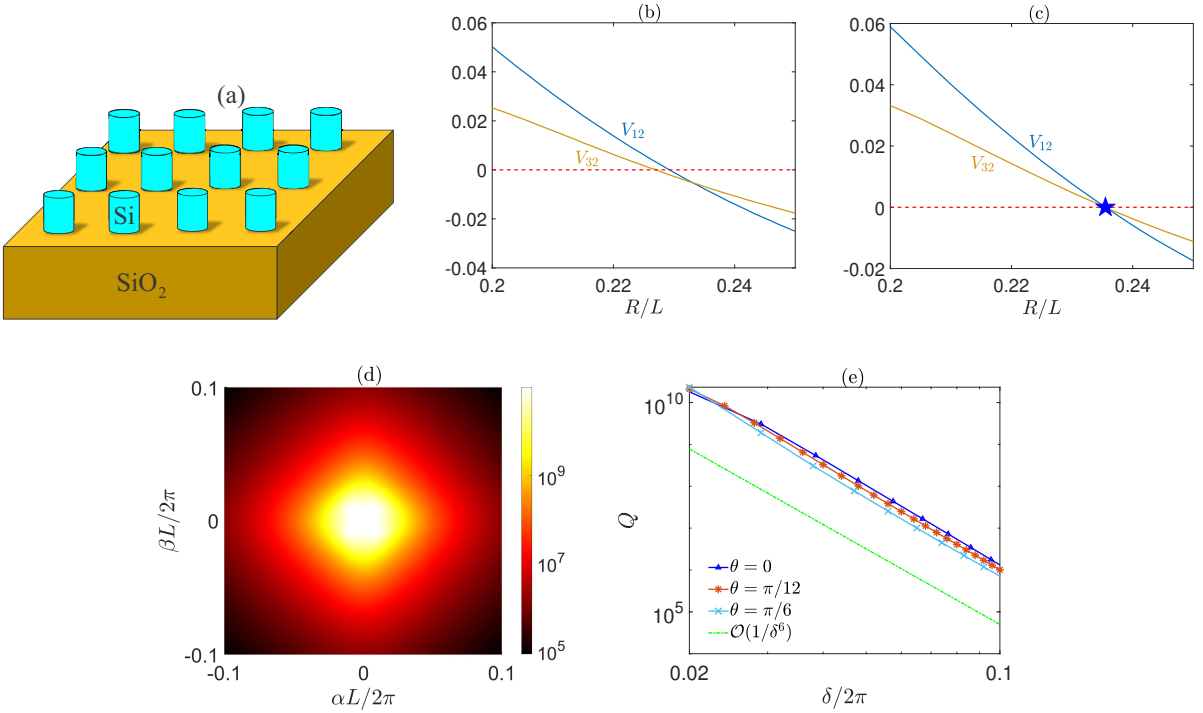


FIG. 3. (a). Schematic of a square lattice of silicon cylinders on a silica substrate. (b) and (c). The quantities  $V_{12}$  and  $V_{21}$  as functions of radius  $R$  for heights  $h = 0.8L$  and  $h = 0.82045L$ , respectively. The blue pentagram corresponds to the super-BIC. (d).  $Q$ -factor of resonant states near a super BIC at  $R = 0.2362L$  and  $h = 0.82045L$ . (e). Asymptotic behavior of  $Q$ -factor in three directions.

BICs where  $\mathbf{d}_1$  is circularly polarized at some angles  $\theta_c$ . In these directions, the resonant states near the BIC are nearly circularly polarized. To determine these BICs and their related angles  $\theta_c$ , we first reduce Eq. (6) to a simpler form

$$\begin{bmatrix} d_{1s} \\ d_{1p} \end{bmatrix} = \tilde{\mathbf{S}}^{1/2} \tilde{\mathbf{V}} \begin{bmatrix} \cos \theta \\ \sin \theta \end{bmatrix}, \quad (8)$$

where  $\tilde{\mathbf{S}}$  is the scattering matrix in a reduced form given by

$$\tilde{\mathbf{S}} = \begin{bmatrix} C_{ss} & C_{ps} \\ C_{sp} & C_{pp} \end{bmatrix} = \mathbf{S}_{11} \pm \mathbf{S}_{21}, \quad \mathbf{S} = \begin{bmatrix} \mathbf{S}_{11} & \mathbf{S}_{12} \\ \mathbf{S}_{21} & \mathbf{S}_{22} \end{bmatrix},$$

where the operation “ $\pm$ ” depends on the up-down mirror symmetry of  $\mathbf{u}_*$ . As shown in Supplementary Material, circularly polarized  $\mathbf{d}_1$  can occur if and only if the scattering coefficients satisfy  $\arg(C_{ss}\overline{C_{pp}}) = \pm\pi$  or  $C_{ss} = C_{pp} = 0$  (polarization conversion). The angles  $\theta_c$  can be solved from the relation  $d_{1s} = \pm id_{1p}$  and Eq. (8).

To validate our theory, we consider a periodic array of circular cylinders with  $\epsilon_c = 4$ . For  $R = 0.2001L$ , we have a BIC in a TE band with  $C_{ss} = -C_{pp} = -0.9590 + 0.2835i$  satisfying  $\arg(C_{ss}\overline{C_{pp}}) = \pi$ . A straightforward calculation gives

$$\tilde{\mathbf{V}} = \begin{bmatrix} 0 & -11.38 \\ -1.064 & 0 \end{bmatrix}$$

and four angles  $\theta_c = \pm 0.09325$  and  $\pm 0.09325 \mp \pi$  at which  $\mathbf{d}_1$  is circularly polarized. The above results are confirmed in Fig. 4(a), showing that  $S_3/S_0 \rightarrow \mp 1$  as  $\delta \rightarrow 0$  for  $\theta_c = \pm 0.09325$ , respectively. Here  $S_0 = |d_s|^2 + |d_p|^2$  and  $S_3 = -2\text{Im}(d_s\overline{d_p})$ . Moreover, as shown in Fig. 4(b), resonant states with  $|S_3/S_0| > 0.5$  can exist in four cone regions induced by these four directions (yellow lines), and the cone angles can be estimated by the polarization vector  $\mathbf{d}_1$ .

If  $\mathbf{d}_1$  is not circularly polarized for all directions, we show that the matrices  $\tilde{\mathbf{S}}$  and  $\tilde{\mathbf{V}}$  can indicate the topological nature of the BIC directly. The Stokes parameters  $S_{1,1}$ ,  $S_{1,2}$  can be written in a compact form

$$\begin{bmatrix} S_{1,1} \\ S_{1,2} \end{bmatrix} = \mathbf{F} \begin{bmatrix} \cos 2\theta \\ \sin 2\theta \end{bmatrix} + \mathbf{g}, \quad (9)$$

where  $\mathbf{F}$  is a real matrix and  $\mathbf{g}$  is a real vector obtained from the definition of Stokes parameters and Eq. (6) directly. As shown in Supplementary Material, the matrix  $\mathbf{F}$  is non-singular if and only if  $\mathbf{d}_1$  is not circularly polarized for all  $\theta$ . In this case, the trajectory  $(S_{1,1}, S_{1,2})$  forms an ellipse with two revolutions around the origin. The revolution direction depends on the matrices  $\tilde{\mathbf{S}}$  and  $\tilde{\mathbf{V}}$ . Therefore, we must have  $\phi_1(2\pi) - \phi_1(0) = \pm 2\pi$  and obtain topological charge  $\pm 1$  directly from  $\phi_1$ .

Finally, we discuss the polarizations near an at- $\Gamma$  BIC in a structure with  $C_{4v}$  symmetry. The matrix  $\tilde{\mathbf{S}}$  is a

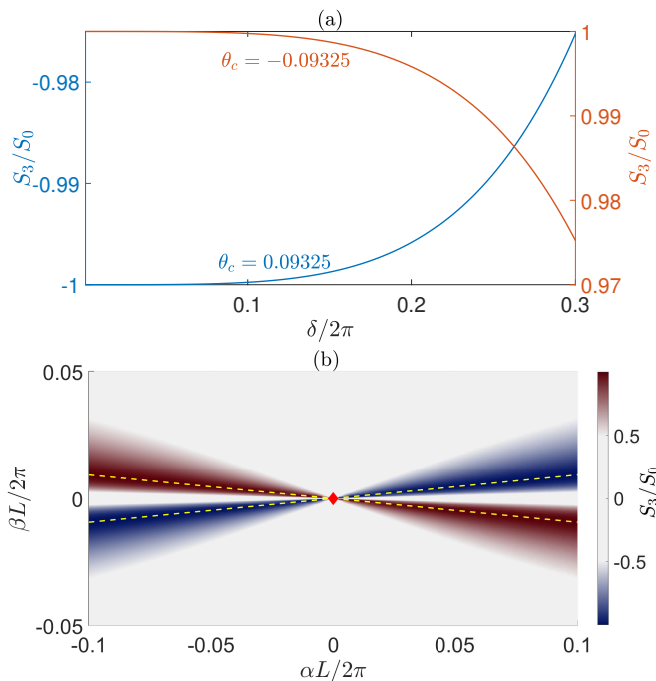


FIG. 4. (a).  $S_3/S_0$  versus  $\delta$  at  $\theta_c = \pm 0.09325$ , respectively. (b).  $S_3/S_0$  in the momentum space. The red diamond represents the BIC. The yellow dash lines represent angles  $\theta_c = \pm 0.09325$  and  $\theta_c = \pm 0.09325 \mp \pi$ .

scalar matrix and  $\tilde{\mathbf{V}}$  has the form of

$$\tilde{\mathbf{V}} = C \begin{bmatrix} 1 & 0 \\ 0 & \pm 1 \end{bmatrix} \text{ or } C \begin{bmatrix} 0 & 1 \\ \pm 1 & 0 \end{bmatrix},$$

where  $C$  is a constant. In this case, the phase difference between  $d_{1s}$  and  $d_{1p}$  is 0 or  $\pi$ , i.e.,  $\mathbf{d}_1$  is linearly polarized. Therefore, resonant states near an at- $\Gamma$  BIC in a structure with  $C_{4v}$  symmetry are nearly linearly polarized.

In summary, we developed a perturbation theory to analyze resonant states near a BIC in PhC slabs, and determined the asymptotic behavior of  $Q$ -factor and the polarization rigorously. Our theory introduces a novel perspective on super-BICs and provides a clear and precise condition for efficiently identifying them in both symmetric and asymmetric structures, without the need to follow a merging process. As an illustrative example, we found a super-BIC in a square lattice of silicon cylinders on a silica substrate. Additionally, we have demonstrated that under a certain condition, the resonant states near the BIC can exhibit nearly circular polarization. The findings presented in this paper may hold direct and potential applications in the fields of resonance and chiral optics. Although the current study has focused on resonant states near a BIC in PhC slabs, our theory can be extended to other systems where BICs exist [55–61].

The authors acknowledge support from the Research Grants Council of Hong Kong Special Administrative Region, China (Grant No. CityU 11304619).

- 
- [1] J. von Neumann and E. Wigner, Über merkwürdige diskrete eigenwerte, *Phys. Z.* **30**, 465 (1929).
- [2] H. Friedrich and D. Wintgen, Interfering resonances and bound states in the continuum, *Phys. Rev. A* **32**, 3231 (1985).
- [3] A.-S. Bonnet-Bendhia and F. Starling, Guided waves by electromagnetic gratings and non-uniqueness examples for the diffraction problem, *Math. Methods Appl. Sci.* **17**, 305 (1994).
- [4] D. V. Evans, M. Levitin, and D. Vassiliev, Existence theorems for trapped modes, *J. Fluid Mech.* **261**, 21 (1994).
- [5] D. C. Marinica, A. G. Borisov, and S. V. Shabanov, Bound States in the Continuum in Photonics, *Phys. Rev. Lett.* **100**, 183902 (2008).
- [6] E. N. Bulgakov and A. F. Sadreev, Bound states in the continuum in photonic waveguides inspired by defects, *Phys. Rev. B* **78**, 075105 (2008).
- [7] Y. Plotnik, O. Peleg, F. Dreisow, M. Heinrich, S. Nolte, A. Szameit, and M. Segev, Experimental Observation of Optical Bound States in the Continuum, *Phys. Rev. Lett.* **107**, 183901 (2011).
- [8] C. W. Hsu, B. Zhen, J. Lee, S.-L. Chua, S. G. Johnson, J. D. Joannopoulos, and M. Soljačić, Observation of trapped light within the radiation continuum, *Nature* **499**, 188 (2013).
- [9] C. W. Hsu, B. Zhen, A. D. Stone, J. D. Joannopoulos, and M. Soljačić, Bound states in the continuum, *Nat. Rev. Mater.* **1**, 16048 (2016).
- [10] K. L. Koshelev, Z. F. Sadrieva, A. A. Shcherbakov, Y. S. Kivshar, and A. A. Bogdanov, Bound states in the continuum in photonic structures, *Phys.-Uspekhi* **93**, 528 (2023).
- [11] S. Fan and J. D. Joannopoulos, Analysis of guided resonances in photonic crystal slabs, *Phys. Rev. B* **65**, 235112 (2002).
- [12] S. P. Shipman and S. Venakides, Resonance and bound states in photonic crystal slabs, *SIAM J. Appl. Math.* **64**, 322 (2003).
- [13] J. Lee, B. Zhen, S.-L. Chua, W. Qiu, J. D. Joannopoulos, M. Soljačić, and O. Shapira, Observation and Differentiation of Unique High- $Q$  Optical Resonances Near Zero Wave Vector in Macroscopic Photonic Crystal Slabs, *Phys. Rev. Lett.* **109**, 067401 (2012).
- [14] V. Mocella and S. Romano, Giant field enhancement in photonic resonant lattices, *Phys. Rev. B* **92**, 155117 (2015).
- [15] A. Kodigala, T. Lepetit, Q. Gu, B. Bahari, Y. Fainman, and B. Kanté, Lasing action from photonic bound states in continuum, *Nature* **541**, 196 (2017).
- [16] A. A. Yanik, A. E. Cetin, M. Huang, A. Artar, S. H. Mousavi, A. Khanikaev, J. H. Connor, G. Shvets, and H. Altug, Seeing protein monolayers with naked eye through plasmonic Fano resonances, *Proc. Natl. Acad. Sci. USA* **108**, 11784 (2011).
- [17] L. Yuan and Y. Y. Lu, Strong resonances on periodic arrays of cylinders and optical bistability with weak in-

- cident waves, *Phys. Rev. A* **95**, 023834 (2017).
- [18] L. Yuan and Y. Y. Lu, Bound states in the continuum on periodic structures surrounded by strong resonances, *Phys. Rev. A* **97**, 043828 (2018).
- [19] J. Jin, X. Yin, L. Ni, M. Soljačić, B. Zhen, and C. Peng, Topologically enabled ultrahigh- $Q$  guided resonances robust to out-of-plane scattering, *Nature* **574**, 501 (2019).
- [20] L. Yuan and Y. Y. Lu, Perturbation theories for symmetry-protected bound states in the continuum on two-dimensional periodic structures, *Phys. Rev. A* **101**, 043827 (2020).
- [21] M. Kang, S. Zhang, M. Xiao, and H. Xu, Merging Bound States in the Continuum at Off-High Symmetry Points, *Phys. Rev. Lett.* **126**, 117402 (2021).
- [22] M.-S. Hwang, H.-C. Lee, K.-H. Kim, K.-Y. Jeong, S.-H. Kwon, K. Koshelev, Y. Kivshar, and H.-G. Park, Ultralow-threshold laser using super-bound states in the continuum, *Nat. Commun.* **12**, 4135 (2021).
- [23] M. Kang, L. Mao, S. Zhang, M. Xiao, H. Xu, and C. T. Chan, Merging bound states in the continuum by harnessing higher-order topological charges, *Light Sci. Appl.* **11**, 228 (2022).
- [24] H. Luo, L. Liu, Z. Xi, Y. Lu, and P. Wang, Dynamics of diverse polarization singularities in momentum space with far-field interference, *Phys. Rev. A* **107**, 013504 (2023).
- [25] E. Bulgakov, G. Shadrina, A. Sadreev, and K. Pichugin, Super-bound states in the continuum through merging in grating, *Phys. Rev. B* **108**, 125303 (2023).
- [26] S.-G. Lee, S.-H. Kim, and W.-J. Lee, Merging and band transition of bound states in the continuum in leaky-mode photonic lattices, *Laser Photonics Rev.* **17**, 2300550 (2023).
- [27] L. Liu, H. Luo, Y. Lu, and P. Wang, Merging diverse bound states in the continuum: from intrinsic to extrinsic scenarios, *Opt. Express* **32**, 16491 (2024).
- [28] N. D. Le, P. Bouteyre, A. Kheir-Aldine, F. Dubois, S. Cuff, L. Berguiga, X. Letartre, P. Viktorovitch, T. Benyattou, and H. S. Nguyen, Super Bound States in the Continuum on a Photonic Flatband: Concept, Experimental Realization, and Optical Trapping Demonstration, *Phys. Rev. Lett.* **132**, 173802 (2024).
- [29] N. Zhang and Y. Y. Lu, Bifurcation of bound states in the continuum in periodic structures, *Opt. Lett.* **49**, 1461 (2024).
- [30] N. Zhang and Y. Y. Lu, Non-generic bound states in the continuum in waveguides with lateral leakage channels, *Opt. Express* **32**, 3764 (2024).
- [31] H. M. Doeleman, F. Monticone, W. den Hollander, A. Alù, and A. F. Koenderink, Experimental observation of a polarization vortex at an optical bound state in the continuum, *Nat. Photon.* **12**, 397 (2018).
- [32] Y. Zhang, A. Chen, W. Liu, C. W. Hsu, B. Wang, F. Guan, X. Liu, L. Shi, L. Lu, and J. Zi, Observation of Polarization Vortices in Momentum Space, *Phys. Rev. Lett.* **120**, 186103 (2018).
- [33] B. Wang, W. Liu, M. Zhao, J. Wang, Y. Zhang, A. Chen, F. Guan, X. Liu, L. Shi, and J. Zi, Generating optical vortex beams by momentum-space polarization vortices centred at bound states in the continuum, *Nat. Photon.* **14**, 623 (2020).
- [34] J. Wang, M. Zhao, W. Liu, F. Guan, X. Liu, L. Shi, C. T. Chan, and J. Zi, Shifting beams at normal incidence via controlling momentum-space geometric phases, *Nat. Commun.* **12**, 6046 (2021).
- [35] B. Zhen, C. W. Hsu, L. Lu, A. D. Stone, and M. Soljačić, Topological Nature of Optical Bound States in the Continuum, *Phys. Rev. Lett.* **113**, 257401 (2014).
- [36] E. N. Bulgakov and D. N. Maksimov, Bound states in the continuum and polarization singularities in periodic arrays of dielectric rods, *Phys. Rev. A* **96**, 063833 (2017).
- [37] W. Liu, B. Wang, Y. Zhang, J. Wang, M. Zhao, F. Guan, X. Liu, L. Shi, and J. Zi, Circularly Polarized States Spawning from Bound States in the Continuum, *Phys. Rev. Lett.* **123**, 116104 (2019).
- [38] W. Chen, Y. Chen, and W. Liu, Singularities and Poincaré Indices of Electromagnetic Multipoles, *Phys. Rev. Lett.* **122**, 153907 (2019).
- [39] T. Yoda and M. Notomi, Generation and Annihilation of Topologically Protected Bound States in the Continuum and Circularly Polarized States by Symmetry Breaking, *Phys. Rev. Lett.* **125**, 053902 (2020).
- [40] W. Chen, Y. Chen, and W. Liu, Line singularities and Hopf indices of electromagnetic multipoles, *Laser Photonics Rev.* **14**, 2000049 (2020).
- [41] W. Liu, W. Liu, L. Shi, and Y. Kivshar, Topological polarization singularities in metaphotonics, *Nanophotonics* **10**, 1469 (2021).
- [42] Q. Jiang, P. Hu, J. Wang, D. Han, and J. Zi, General Bound States in the Continuum in Momentum Space, *Phys. Rev. Lett.* **131**, 013801 (2023).
- [43] L. Zagaglia, S. Zanotti, M. Minkov, M. Liscidini, D. Gerace, and L. C. Andreani, Polarization states and far-field optical properties in dielectric photonic crystal slabs, *Opt. Lett.* **48**, 5017 (2023).
- [44] Z. Zhao, C. Guo, and S. Fan, Connection of temporal coupled-mode-theory formalisms for a resonant optical system and its time-reversal conjugate, *Phys. Rev. A* **99**, 033839 (2019).
- [45] R. Kazarinov and C. Henry, Second-order distributed feedback lasers with mode selection provided by first-order radiation losses, *IEEE J. Quantum Electron.* **21**, 144 (1985).
- [46] X. Zhang, Y. Liu, J. Han, Y. Kivshar, and Q. Song, Chiral emission from resonant metasurfaces, *Science* **377**, 1215 (2022).
- [47] L. Liu, H. Luo, Z. Xi, Y. Lu, and P. Wang, Ultrahigh- $Q$  and angle-robust chiroptical resonances beyond BIC splitting, *Opt. Lett.* **49**, 153 (2024).
- [48] Y. Chen, H. Deng, X. Sha, W. Chen, R. Wang, Y.-H. Chen, D. Wu, J. Chu, Y. S. Kivshar, S. Xiao, and C.-W. Qiu, Observation of intrinsic chiral bound states in the continuum, *Nature* **613**, 474 (2023).
- [49] Y. Chen, W. Chen, X. Kong, D. Wu, J. Chu, and C.-W. Qiu, Can Weak Chirality Induce Strong Coupling Between Resonant States?, *Phys. Rev. Lett.* **128**, 146102 (2022).
- [50] X. Zhao, J. Wang, W. Liu, Z. Che, X. Wang, C. T. Chan, L. Shi, and J. Zi, Spin-Orbit-Locking Chiral Bound States in the Continuum, *Phys. Rev. Lett.* **133**, 036201 (2024).
- [51] E. N. Bulgakov and D. N. Maksimov, Bound states in the continuum and Fano resonances in the Dirac cone spectrum, *J. Opt. Soc. Am. B* **36**, 2221 (2019).
- [52] A. S. Kostyukov, V. S. Gerasimov, A. E. Ersho, and E. N. Bulgakov, Ring of bound states in the continuum in the reciprocal space of a monolayer of high-contrast dielectric spheres, *Phys. Rev. B* **105**, 075404 (2022).

- [53] T. Ochiai, Generation of multiple bound states in the continuum through doubly degenerate quasi-guided modes (2024), arXiv:2404.16472 [physics.optics].
- [54] K. Sakoda, *Optical properties of photonic crystals*, Vol. 2 (Springer, Berlin, 2005).
- [55] X. Gao, B. Zhen, M. Soljačić, H. Chen, and C. W. Hsu, Bound states in the continuum in fiber bragg gratings, *ACS Photonics* **96**, 2996 (2019).
- [56] E. N. Bulgakov and A. F. Sadreev, Bound states in the continuum with high orbital angular momentum in a dielectric rod with periodically modulated permittivity, *Phys. Rev. A* **96**, 013841 (2017).
- [57] N. Zhang and Y. Y. Lu, Robust and non-robust bound states in the continuum in rotationally symmetric periodic waveguides, *Opt. Express* **31**, 15810 (2023).
- [58] M. A. Webster, R. M. Pafchek, A. Mitchell, and T. L. Koch, Width dependence of inherent TM-mode lateral leakage loss in silicon-on-insulator ridge waveguides, *IEEE Photonics Technol. Lett.* **19**, 429 (2007).
- [59] C.-L. Zou, J.-M. Cui, F.-W. Sun, X. Xiong, X.-B. Zou, Z.-F. Han, and G.-C. Guo, Guiding light through optical bound states in the continuum for ultrahigh- $Q$  microresonators, *Laser Photonics Rev.* **9**, 114 (2015).
- [60] L. Yuan and Y. Y. Lu, On the robustness of bound states in the continuum in waveguides with lateral leakage channels, *Opt. Express* **29**, 16695 (2021).
- [61] J. Gomis-Bresco, D. Artigas, and L. Torner, Anisotropy-induced photonic bound states in the continuum, *Nat. Photon.* **11**, 232 (2017).
- [62] K. Sakoda, Proof of the universality of mode symmetries in creating photonic dirac cones, *Opt. Express* **20**, 25181 (2012).
- [63] L. Yuan and Y. Y. Lu, Propagating bloch modes above the lightline on a periodic array of cylinders, *J. Phys. B* **50**, 05LT01 (2017).
- [64] N. Zhang and Y. Y. Lu, An efficient method for calculating resonant modes in biperiodic photonic structures, arXiv, 2403.04459 (2024).

## Supplementary Material

### S1. DERIVATIONS OF EQUATIONS (5) AND (6)

The wave equation for resonant states can be written as

$$\mathcal{L}\mathbf{u} = k^2\varepsilon(\boldsymbol{\rho}, z)\mathbf{u}, \quad (\text{S10})$$

where  $k = \omega/c$  is the free space wavenumber,  $\omega$  is the angular frequency, and  $c$  is the speed of light in vacuum. The wavenumber of resonant states near a BIC can be expanded as

$$k = k_* + \delta k_1(\theta) + \delta^2 k_2(\theta) + \dots \quad (\text{S11})$$

Substituting Eqs. (3)-(4) and (S11) into Eq. (S10) and collecting the  $\mathcal{O}(\delta)$  terms, we obtain the 1st-order perturbation equation

$$\mathcal{M}_*\mathbf{u}_1 = [2k_*k_1\varepsilon - \mathcal{L}_1(\theta)]\mathbf{u}_*, \quad (\text{S12})$$

where  $\mathcal{M}_* = \mathcal{L}_* - k_*^2\varepsilon$  is the wave operator. To study the solutions of Eq. (S12), we introduce some mathematical theories as follows. For convenience, we first restate Green's theorem here:

$$\iint_V (\mathbf{w} \cdot \nabla \times \nabla \times \mathbf{v} - \mathbf{v} \cdot \nabla \times \nabla \times \mathbf{w}) \, dV = \int_S (\mathbf{v} \times \nabla \times \mathbf{w} - \mathbf{w} \times \nabla \times \mathbf{v}) \cdot \mathbf{n} \, dS,$$

and

$$\iint_V (\mathbf{w} \cdot \nabla \times \mathbf{v} - \mathbf{v} \cdot \nabla \times \mathbf{w}) \, dV = \int_S (\mathbf{n} \times \mathbf{v}) \cdot \mathbf{u} \, dS,$$

where  $V$  is a domain with the boundary  $S$ ,  $\mathbf{n}$  is the outward unit normal vector of  $S$ ,  $\mathbf{w}$  and  $\mathbf{v}$  are vector functions. A differential equation  $\mathcal{M}_*\mathbf{v} = \mathbf{w}$  is solvable if and only if  $\langle \mathbf{u}_* | \mathbf{w} \rangle = 0$ . Here  $\langle \mathbf{w} | \mathbf{v} \rangle$  is an inner product defined by

$$\langle \mathbf{w} | \mathbf{v} \rangle = \frac{1}{L^3} \int_{\Omega} \overline{\mathbf{w}} \cdot \mathbf{v} \, dx dy dz,$$

where  $\Omega = (-L/2, L/2) \times (-L/2, L/2) \times \mathbb{R}$  is a unit cell and  $\overline{\mathbf{w}}$  represents the complex conjugate of  $\mathbf{w}$ . If the source term  $\mathbf{w}$  vanishes in the far-field, i.e.,  $\mathbf{w} \rightarrow 0$  as  $z \rightarrow \pm\infty$ , according to the far-field pattern of the Green's function, all solutions  $\mathbf{v}$  must satisfy  $\mathbf{v} \sim \mathbf{e}^{\pm i\gamma_*^\pm z}$  as  $z \rightarrow \pm\infty$ .

The solvability condition for Eq. (S12) leads to  $2k_*k_1 = \langle \mathbf{u}_* | \mathcal{L}_1 | \mathbf{u}_* \rangle$ , where

$$\langle \mathbf{w} | \mathcal{L}_1 | \mathbf{v} \rangle = \frac{1}{L^3} \int_{\Omega} \overline{\mathbf{w}} \cdot \mathcal{L}_1 \mathbf{v} \, dx dy dz.$$

By Green's theorem, we show that  $k_1$  is real. In addition, all solutions  $\mathbf{u}_1$  satisfy the asymptotic behavior

$$\mathbf{u}_1 \sim \mathbf{d}_1^\pm e^{\pm i\gamma_*^\pm z}, \quad z \rightarrow \pm\infty. \quad (\text{S13})$$

Substituting Eqs. (3)-(4), (S11) and (S13) into Gauss's law  $(\nabla + i\boldsymbol{\alpha}) \cdot \mathbf{u} = 0$  and collecting the  $\mathcal{O}(\delta)$  terms, we obtain  $\mathbf{k}_*^\pm \cdot \mathbf{d}_1^\pm = 0$ , where  $\mathbf{k}_*^\pm = (\alpha_*, \beta_*, \pm\gamma_*^\pm)$ . Thus the vectors  $\mathbf{d}_1^\pm$  can be decomposed as  $\mathbf{d}_1^\pm = d_{1s}^\pm \hat{\mathbf{s}}_* + d_{1p}^\pm \hat{\mathbf{p}}_*^\pm$ , where,

$$\hat{\mathbf{s}}_* = \begin{cases} \frac{\hat{z} \times \mathbf{k}_*^\pm}{|\hat{z} \times \mathbf{k}_*^\pm|}, & \hat{z} \times \mathbf{k}_*^\pm \neq 0 \\ \hat{x}, & \hat{z} \times \mathbf{k}_*^\pm = 0 \end{cases}, \quad \hat{\mathbf{p}}_*^\pm = \pm \mathbf{k}_*^\pm \times \hat{\mathbf{s}}_*/k_*.$$

Collecting the  $\mathcal{O}(\delta^2)$  terms in Eq. (S10), we can obtain

$$\mathcal{M}_* \mathbf{u}_2 = (2k_* k_1 \varepsilon - \mathcal{L}_1) \mathbf{u}_1 + [(k_1^2 + 2k_* k_2) \varepsilon - \mathcal{L}_2] \mathbf{u}_*. \quad (\text{S14})$$

The solvability condition for Eq. (S14) gives rise to

$$\text{Im}(2k_* k_2) = -\text{Im} \langle \mathbf{u}_* | 2k_* k_1 \varepsilon - \mathcal{L}_1 | \mathbf{u}_1 \rangle = \text{Im} \langle \mathbf{u}_1 | \mathcal{M}_* | \mathbf{u}_1 \rangle.$$

Since  $\text{Im} \langle \mathbf{u}_1 | \mathcal{M}_* | \mathbf{u}_1 \rangle = (\langle \mathbf{u}_1 | \mathcal{L}_* | \mathbf{u}_1 \rangle - \overline{\langle \mathbf{u}_1 | \mathcal{L}_* | \mathbf{u}_1 \rangle}) / 2i$ , by using Green's theorem and the asymptotic behavior of  $\mathbf{u}_1$ , we obtain Eq. (5) in the Letter.

To calculate  $\mathbf{d}_1^\pm$ , we introduce four linearly independent diffraction solutions. We denote several plane waves by

$$\mathbf{s}^\pm = \eta^\pm \hat{\mathbf{s}} e^{\pm i\gamma_*^\pm z}, \quad \mathbf{p}_s^\pm = \eta^\pm \hat{\mathbf{p}}^\pm e^{\pm i\gamma_*^\pm z}, \quad \mathbf{p}_i^\pm = -\mathcal{C}_2 \mathbf{p}_s^\pm,$$

where  $\eta^\pm = \sqrt{k_*/\gamma_*^\pm}$  are used to normalize the power. When the structure is illuminated by incident plane waves  $\bar{\mathbf{s}}^\pm$  and  $\bar{\mathbf{p}}_i^\pm$  in the upper and lower regions, respectively, we obtain four linearly independent diffraction solutions  $\tilde{\mathbf{u}}_{s*}^\pm$  and  $\tilde{\mathbf{u}}_{p*}^\pm$  satisfying the asymptotic behavior

$$\tilde{\mathbf{u}}_{s*}^+ \sim \begin{cases} \bar{\mathbf{s}}^+ + R_{ss}^+ \mathbf{s}^+ + R_{ps}^+ \mathbf{p}_s^+, & z \rightarrow +\infty \\ T_{ss}^+ \mathbf{s}^- + T_{ps}^+ \mathbf{p}_s^-, & z \rightarrow -\infty \end{cases}, \quad \tilde{\mathbf{u}}_{p*}^+ \sim \begin{cases} \bar{\mathbf{p}}_i^+ + R_{sp}^+ \mathbf{s}^+ + R_{pp}^+ \mathbf{p}_s^+, & z \rightarrow +\infty \\ T_{sp}^+ \mathbf{s}^- + T_{pp}^+ \mathbf{p}_s^-, & z \rightarrow -\infty \end{cases}$$

$$\tilde{\mathbf{u}}_{s*}^- \sim \begin{cases} T_{ss}^- \mathbf{s}^+ + T_{ps}^- \mathbf{p}_s^+, & z \rightarrow +\infty \\ \bar{\mathbf{s}}^- + R_{ss}^- \mathbf{s}^- + R_{ps}^- \mathbf{p}_s^-, & z \rightarrow -\infty \end{cases}, \quad \tilde{\mathbf{u}}_{p*}^- \sim \begin{cases} T_{sp}^- \mathbf{s}^+ + T_{pp}^- \mathbf{p}_s^+, & z \rightarrow +\infty \\ \bar{\mathbf{p}}_i^- + R_{sp}^- \mathbf{s}^- + R_{pp}^- \mathbf{p}_s^-, & z \rightarrow -\infty \end{cases}.$$

Since  $\mathcal{M}_* \tilde{\mathbf{u}}_{l*}^\pm = 0$ ,  $l \in \{s, p\}$ , we have

$$\langle \tilde{\mathbf{u}}_{l*}^\pm | \mathcal{M}_* | \mathbf{u}_1 \rangle = \langle \tilde{\mathbf{u}}_{l*}^\pm | \mathcal{M}_* | \mathbf{u}_1 \rangle - \langle \mathbf{u}_1 | \mathcal{M}_* | \tilde{\mathbf{u}}_{l*}^\pm \rangle = \langle \tilde{\mathbf{u}}_{l*}^\pm | \mathcal{L}_* | \mathbf{u}_1 \rangle - \langle \mathbf{u}_1 | \mathcal{L}_* | \tilde{\mathbf{u}}_{l*}^\pm \rangle.$$

A straightforward calculation shows that

$$\frac{iL}{2} \langle \tilde{\mathbf{u}}_{s*}^+ | \mathcal{M}_* | \mathbf{u}_1 \rangle = \gamma_*^+ \eta^+ (\bar{R}_{ss}^+ d_{1s}^+ + \bar{R}_{ps}^+ d_{1p}^+) + \gamma_*^- \eta^- (\bar{T}_{ss}^+ d_{1s}^- + \bar{T}_{ps}^+ d_{1p}^-)$$

$$\frac{iL}{2} \langle \tilde{\mathbf{u}}_{p*}^+ | \mathcal{M}_* | \mathbf{u}_1 \rangle = \gamma_*^+ \eta^+ (\bar{R}_{sp}^+ d_{1s}^+ + \bar{R}_{pp}^+ d_{1p}^+) + \gamma_*^- \eta^- (\bar{T}_{sp}^+ d_{1s}^- + \bar{T}_{pp}^+ d_{1p}^-)$$

$$\frac{iL}{2} \langle \tilde{\mathbf{u}}_{s*}^- | \mathcal{M}_* | \mathbf{u}_1 \rangle = \gamma_*^+ \eta^+ (\bar{T}_{ss}^- d_{1s}^+ + \bar{T}_{ps}^- d_{1p}^+) + \gamma_*^- \eta^- (\bar{R}_{ss}^- d_{1s}^- + \bar{R}_{ps}^- d_{1p}^-)$$

$$\frac{iL}{2} \langle \tilde{\mathbf{u}}_{p*}^- | \mathcal{M}_* | \mathbf{u}_1 \rangle = \gamma_*^+ \eta^+ (\bar{T}_{sp}^- d_{1s}^+ + \bar{T}_{pp}^- d_{1p}^+) + \gamma_*^- \eta^- (\bar{R}_{sp}^- d_{1s}^- + \bar{R}_{pp}^- d_{1p}^-).$$

We denote  $-i\tilde{\mathbf{u}}_{l*}^\pm / 2\sqrt{k_* L}$  by  $\mathbf{u}_{l*}^\pm$  and rewrite the above equations in a compact form

$$\begin{bmatrix} d_{1s}^+ \\ d_{1p}^+ \\ d_{1s}^- \\ d_{1p}^- \end{bmatrix} = L^2 \mathbf{\Gamma}^{-1/2} \mathbf{S} \begin{bmatrix} \langle \mathbf{u}_{s*}^+ | \mathcal{M}_* | \mathbf{u}_1 \rangle \\ \langle \mathbf{u}_{p*}^+ | \mathcal{M}_* | \mathbf{u}_1 \rangle \\ \langle \mathbf{u}_{s*}^- | \mathcal{M}_* | \mathbf{u}_1 \rangle \\ \langle \mathbf{u}_{p*}^- | \mathcal{M}_* | \mathbf{u}_1 \rangle \end{bmatrix},$$



where  $\mathbf{\Gamma} = \text{diag}(\gamma_*^+, \gamma_*^+, \gamma_*^-, \gamma_*^-)L$  and  $\mathbf{S}$  is the scattering matrix given by

$$\mathbf{S} = \begin{bmatrix} R_{ss}^+ & R_{sp}^+ & T_{ss}^- & T_{sp}^- \\ R_{ps}^+ & R_{pp}^+ & T_{ps}^- & T_{pp}^- \\ T_{ss}^+ & T_{sp}^+ & R_{ss}^- & R_{sp}^- \\ T_{ps}^+ & T_{pp}^+ & R_{ps}^- & R_{pp}^- \end{bmatrix}.$$

If we shift the diffraction solutions such that they are orthogonal with the BIC, i.e.,  $\langle \mathbf{u}_{l_*}^\pm | \varepsilon | \mathbf{u}_* \rangle = 0$ , according to Eq. (S12), we obtain Eq. (6) in the Letter, i.e.

$$\begin{bmatrix} d_{1s}^+ \\ d_{1p}^+ \\ d_{1s}^- \\ d_{1p}^- \end{bmatrix} = L^2 \mathbf{\Gamma}^{-1/2} \mathbf{S} \begin{bmatrix} \langle \mathbf{u}_{s_*}^+ | \mathcal{L}_1 | \mathbf{u}_* \rangle \\ \langle \mathbf{u}_{p_*}^+ | \mathcal{L}_1 | \mathbf{u}_* \rangle \\ \langle \mathbf{u}_{s_*}^- | \mathcal{L}_1 | \mathbf{u}_* \rangle \\ \langle \mathbf{u}_{p_*}^- | \mathcal{L}_1 | \mathbf{u}_* \rangle \end{bmatrix}.$$

For a super-BIC with vanishing  $\mathbf{d}_1^\pm$ , by using the same procedure, we obtain

$$\mathbf{u}_2 \sim \mathbf{d}_2^\pm e^{\pm i \gamma_*^\pm z}, \quad z \rightarrow \pm \infty.$$

We also have  $\mathbf{k}_*^\pm \cdot \mathbf{d}_2^\pm = 0$  and the vectors  $\mathbf{d}_2^\pm$  can be calculated from

$$\begin{bmatrix} d_{2s}^+ \\ d_{2p}^+ \\ d_{2s}^- \\ d_{2p}^- \end{bmatrix} = L^2 \mathbf{\Gamma}^{-1/2} \mathbf{S} \begin{bmatrix} \langle \mathbf{u}_{s_*}^+ | \mathcal{M}_* | \mathbf{u}_2 \rangle \\ \langle \mathbf{u}_{p_*}^+ | \mathcal{M}_* | \mathbf{u}_2 \rangle \\ \langle \mathbf{u}_{s_*}^- | \mathcal{M}_* | \mathbf{u}_2 \rangle \\ \langle \mathbf{u}_{p_*}^- | \mathcal{M}_* | \mathbf{u}_2 \rangle \end{bmatrix}. \quad (\text{S15})$$

If  $\mathbf{d}_2^\pm \neq 0$ , we have  $2k_* \text{Im}(k_4)L = -(\gamma_*^+ |\mathbf{d}_2^+|^2 + \gamma_*^- |\mathbf{d}_2^-|^2)$ . As  $\delta \rightarrow 0$ , we have  $Q \sim 1/\delta^4$  and  $\mathbf{d} \sim \delta^2 \mathbf{d}_2^\pm$ . If  $\mathbf{d}_2^\pm = 0$ , we can use the same procedure to determine the asymptotic behavior of  $Q$ -factor and polarizations of resonant states near a BIC by higher order state corrections.

## S2. STRUCTURES WITH AN INVERSION SYMMETRY

In this section we show that  $\mathbf{V} = \mathbf{S}^{1/2} \mathbf{U}$  is a real matrix in a structure with an in-plane inversion symmetry. We first construct special diffraction solutions which are linear combinations of  $\mathbf{u}_{s_*}^\pm$  and  $\mathbf{u}_{p_*}^\pm$  and satisfy

$$-C_2 (\bar{a}_s^+ \bar{\mathbf{u}}_{s_*}^+ + \bar{a}_p^+ \bar{\mathbf{u}}_{p_*}^+ + \bar{a}_s^- \bar{\mathbf{u}}_{s_*}^- + \bar{a}_p^- \bar{\mathbf{u}}_{p_*}^-) = a_s^+ \mathbf{u}_{s_*}^+ + a_p^+ \mathbf{u}_{p_*}^+ + a_s^- \mathbf{u}_{s_*}^- + a_p^- \mathbf{u}_{p_*}^-, \quad (\text{S16})$$

where  $a_s^\pm$  and  $a_p^\pm$  are four undetermined coefficients. Since the left and right terms in Eq. (S16) must have the same far-field patterns, we have

$$\mathbf{S} \mathbf{a} = \bar{\mathbf{a}}, \quad \mathbf{a} = \begin{bmatrix} a_s^+ \\ a_p^+ \\ a_s^- \\ a_p^- \end{bmatrix}.$$

In a structure with an inversion symmetry, the scattering matrix is unitary and symmetric, i.e.,  $\mathbf{S}^* \mathbf{S} = \mathbf{I}$  and  $\mathbf{S} = \mathbf{S}^\top$ . Denoting the eigenvalues and eigenvectors of  $\mathbf{S}$  by  $\lambda_j = \exp(i\phi_j)$  and  $\mathbf{q}_j$ ,  $j = 1, 2, 3, 4$ , we have  $\bar{\lambda}_j \mathbf{q}_j = \mathbf{S}^{-1} \mathbf{q}_j = \bar{\mathbf{S}} \mathbf{q}_j$  and obtain  $\mathbf{S} \bar{\mathbf{q}}_j = \lambda_j \bar{\mathbf{q}}_j$ . Therefore, the eigenvectors can be scaled as real unit vectors that are still denoted by  $\mathbf{q}_j$ . The scattering matrix  $\mathbf{S}$  is diagonalizable and we have

$$\mathbf{S} = \mathbf{Q} \begin{bmatrix} \lambda_1 & & & \\ & \lambda_2 & & \\ & & \lambda_3 & \\ & & & \lambda_4 \end{bmatrix} \mathbf{Q}^\top, \quad \mathbf{Q} = [\mathbf{q}_1, \mathbf{q}_2, \mathbf{q}_3, \mathbf{q}_4].$$

Moreover, we have

$$\mathbf{S}^{\pm 1/2} = \mathbf{Q} \begin{bmatrix} \lambda_1^{\pm 1/2} & & & \\ & \lambda_2^{\pm 1/2} & & \\ & & \lambda_3^{\pm 1/2} & \\ & & & \lambda_4^{\pm 1/2} \end{bmatrix} \mathbf{Q}^\top,$$

and  $\bar{\mathbf{S}}^{-1/2} = \mathbf{S}^{1/2}$ . Let  $[\mathbf{a}_1, \mathbf{a}_2, \mathbf{a}_3, \mathbf{a}_4] = \mathbf{S}^{-1/2}$ , we obtain four diffraction solutions

$$\mathbf{u}_*^l = a_{ls}^+ \mathbf{u}_{s*}^+ + a_{lp}^+ \mathbf{u}_{p*}^+ + a_{ls}^- \mathbf{u}_{s*}^- + a_{lp}^- \mathbf{u}_{p*}^-, \quad l = 1, 2, 3, 4$$

satisfying  $\mathcal{C}_2 \bar{\mathbf{u}}_*^l = -\mathbf{u}_*^l$ ,  $1 \leq l \leq 4$ . Since  $\bar{\mathcal{L}}_1 = -\mathcal{L}_1$  and

$$\mathcal{C}_2(\overline{\mathcal{L}_1 \mathbf{u}_*}) = -\mathcal{C}_2(\mathcal{L}_1 \bar{\mathbf{u}}_*) = \mathcal{L}_1 \mathcal{C}_2 \bar{\mathbf{u}}_* = -\mathcal{L}_1 \mathbf{u}_*,$$

we obtain real qualities  $L^2 \langle \mathbf{u}_*^l | \mathcal{L}_1 | \mathbf{u}_* \rangle$ . Consequently, the matrix  $\mathbf{V} = \mathbf{S}^{1/2} \mathbf{U} = (\mathbf{S}^{-1/2})^* \mathbf{U}$  is real.

### S3. SUPER-BICS IN STRUCTURES WITH $C_{4v}$ SYMMETRY

In this section we show that for at- $\Gamma$  super-BICs in structures with  $C_{4v}$  symmetry, we typically have  $Q \sim 1/\delta^6$  in all directions. Equivalently, we prove that  $\mathbf{d}_1^\pm = \mathbf{d}_2^\pm = 0$  for all  $\theta$ . As an illustration, we consider a non-degenerate BIC belonging to  $A_2$  representation. The four diffraction solutions  $\mathbf{u}_{s*}^\pm$  and  $\mathbf{u}_{p*}^\pm$  belong to  $E$  representation [54, 62]. Our theory remains valid for BICs belonging to other representations.

The solvability condition for Eq. (S12) gives rise to  $k_1 = 0$  since  $\mathcal{C}_2 \mathcal{L}_1 = -\mathcal{C}_2 \mathcal{L}_1$  and  $\langle \mathbf{u}_* | \mathcal{L}_1 | \mathbf{u}_* \rangle = 0$ . According the symmetries of  $\mathbf{u}_*$  and  $\mathbf{u}_{l*}^\pm$ , we have  $\langle \mathbf{u}_{s*}^\pm | \mathcal{L}_{1x} | \mathbf{u}_* \rangle = \langle \mathbf{u}_{p*}^\pm | \mathcal{L}_{1y} | \mathbf{u}_* \rangle$  and  $\langle \mathbf{u}_{s*}^\pm | \mathcal{L}_{1y} | \mathbf{u}_* \rangle = -\langle \mathbf{u}_{p*}^\pm | \mathcal{L}_{1x} | \mathbf{u}_* \rangle$ . Moreover, we have

$$\langle \mathbf{u}_{s*}^\pm | \mathcal{L}_{1x} | \mathbf{u}_* \rangle = -\langle \sigma_x \mathbf{u}_{s*}^\pm | \sigma_x \mathcal{L}_{1x} | \mathbf{u}_* \rangle = \langle \mathbf{u}_{s*}^\pm | \mathcal{L}_{1x} \sigma_x | \mathbf{u}_* \rangle = -\langle \mathbf{u}_{s*}^\pm | \mathcal{L}_{1x} | \mathbf{u}_* \rangle = 0,$$

where  $\sigma_x$  is a symmetry operator related to reflection symmetry in  $x$ . Therefore, we have

$$\mathbf{U}^\pm = L^2 \begin{bmatrix} 0 & \langle \mathbf{u}_{s*}^\pm | \mathcal{L}_{1y} | \mathbf{u}_* \rangle \\ \langle \mathbf{u}_{p*}^\pm | \mathcal{L}_{1x} | \mathbf{u}_* \rangle & 0 \end{bmatrix}.$$

Since cross polarization cannot occur, we have

$$\mathbf{V} = \begin{bmatrix} 0 & V_{12} \\ -V_{12} & 0 \\ 0 & V_{32} \\ -V_{32} & 0 \end{bmatrix}.$$

If the BIC is a super-BIC,  $\mathbf{V}$  is rank-deficient and we have  $V_{12} = V_{32} = 0$ . Thus,  $\mathbf{d}_1^\pm = 0$  for all  $\theta$ . Next, we prove that  $\mathbf{d}_2^\pm = 0$  in all directions. The solutions  $\mathbf{u}_1$  can be written as

$$\mathbf{u}_1 = \mathbf{u}_{1x} \cos \theta + \mathbf{u}_{1y} \sin \theta, \quad (\text{S17})$$

where

$$\mathcal{M}_* \mathbf{u}_{1x} = -\mathcal{L}_{1x} \mathbf{u}_*, \quad \mathcal{M}_* \mathbf{u}_{1y} = -\mathcal{L}_{1y} \mathbf{u}_*.$$

Substituting Eq. (S17) into Eq. (S14), we have

$$\mathcal{M}_* \mathbf{u}_2 = 2k_* k_2 \varepsilon \mathbf{u}_* + (\mathcal{L}_{1x} \cos \theta + \mathcal{L}_{1y} \sin \theta)(\mathbf{u}_{1x} \cos \theta + \mathbf{u}_{1y} \sin \theta) - \mathcal{L}_2 \mathbf{u}_*.$$

The vectors  $\mathbf{d}_2^\pm$  can be calculated from Eq. (S15) and

$$\begin{aligned} \langle \mathbf{u}_{s*}^\pm | \mathcal{M}_* | \mathbf{u}_2 \rangle &= [\cos \theta, \sin \theta] \begin{bmatrix} \langle \mathbf{u}_{s*}^\pm | \mathcal{L}_{1x} | \mathbf{u}_{1x} \rangle & \langle \mathbf{u}_{s*}^\pm | \mathcal{L}_{1x} | \mathbf{u}_{1y} \rangle \\ \langle \mathbf{u}_{s*}^\pm | \mathcal{L}_{1y} | \mathbf{u}_{1x} \rangle & \langle \mathbf{u}_{s*}^\pm | \mathcal{L}_{1y} | \mathbf{u}_{1y} \rangle \end{bmatrix} \begin{bmatrix} \cos \theta \\ \sin \theta \end{bmatrix} \\ \langle \mathbf{u}_{p*}^\pm | \mathcal{M}_* | \mathbf{u}_2 \rangle &= [\cos \theta, \sin \theta] \begin{bmatrix} \langle \mathbf{u}_{p*}^\pm | \mathcal{L}_{1x} | \mathbf{u}_{1x} \rangle & \langle \mathbf{u}_{p*}^\pm | \mathcal{L}_{1x} | \mathbf{u}_{1y} \rangle \\ \langle \mathbf{u}_{p*}^\pm | \mathcal{L}_{1y} | \mathbf{u}_{1x} \rangle & \langle \mathbf{u}_{p*}^\pm | \mathcal{L}_{1y} | \mathbf{u}_{1y} \rangle \end{bmatrix} \begin{bmatrix} \cos \theta \\ \sin \theta \end{bmatrix}. \end{aligned}$$

Since  $\mathcal{C}_2 \mathcal{L}_{1\sigma} \mathbf{u}_{1\kappa} = \mathcal{L}_{1\sigma} \mathbf{u}_{1\kappa}$ ,  $\sigma, \kappa \in \{x, y\}$ , the matrices shown in the above formulas are zero. Thus,  $\mathbf{d}_2^\pm = 0$  and  $Q \sim 1/\delta^6$  for all  $\theta$  at least. For super-BICs in a structure with an inversion symmetry (e.g., a periodic array of cylinders), our theory applies these cases as well.

#### S4. NEARLY CIRCULARLY POLARIZED AND TOPOLOGICAL NATURES

In this section, we study polarizations of resonant states near a generic BIC in structures with an in-plane inversion symmetry and up-down mirror symmetry. We determine BICs and related angles where nearly circular polarizations can occur. If nearly circular polarization cannot occur, we show that the topological charge of BICs must be  $\pm 1$ . For convenience, we remove the symbol “ $\sim$ ” of matrices  $\tilde{\mathbf{S}}$  and  $\tilde{\mathbf{V}}$  in Eq. (8).

The scattering matrix  $\mathbf{S}$  is unitary and symmetric, and can be written as

$$\mathbf{S} = e^{i\kappa} \begin{bmatrix} \frac{\rho e^{i\psi}}{\sqrt{1-\rho^2}} & \sqrt{1-\rho^2} \\ \sqrt{1-\rho^2} & -\rho e^{-i\psi} \end{bmatrix},$$

where  $0 \leq \rho \leq 1$  and  $0 \leq \kappa, \psi \leq 2\pi$ . Since

$$d_{1s}^2 + d_{1p}^2 = [\cos \theta \quad \sin \theta] \mathbf{V}^T \mathbf{S} \mathbf{V} \begin{bmatrix} \cos \theta \\ \sin \theta \end{bmatrix},$$

we show that  $d_{1s}^2 + d_{1p}^2 = 0$  at an angle  $\theta_c$  if and only if

$$\mathbf{v}_c^T \begin{bmatrix} \frac{\rho \cos \psi}{\sqrt{1-\rho^2}} & \sqrt{1-\rho^2} \\ \sqrt{1-\rho^2} & -\rho \cos \psi \end{bmatrix} \mathbf{v}_c = 0 \quad (\text{S18})$$

and

$$\rho \sin \psi \|\mathbf{v}_c\|_2^2 = 0, \quad \mathbf{v}_c = \mathbf{V} \begin{bmatrix} \cos \theta_c \\ \sin \theta_c \end{bmatrix}. \quad (\text{S19})$$

On the other hand, Eqs. (S18) and (S19) have nonzero solutions  $\mathbf{v}_c$  if and only if  $\rho \sin \psi = 0$ . Therefore, for a generic BIC, there exist special angles at which  $\mathbf{d}_1$  is circularly polarized if and only if  $\rho \sin \psi = 0$ , i.e.,  $C_{ss} = C_{pp} = 0$  or  $\arg(C_{ss} \overline{C_{pp}}) = \pm\pi$ . These angles can be solved from the above equations.

Next, we show that if nearly circular polarization cannot occur, the topological charge of the BIC must be  $\pm 1$ . The matrix  $\mathbf{F}$  and the vector  $\mathbf{g}$  in Eq. (9) can be obtained from Eq. (6) and the definition of Stokes parameters directly. Since the matrix  $\mathbf{S}^{1/2}$  is also unitary and symmetric, we have

$$\mathbf{S}^{1/2} = e^{i\tilde{\kappa}} \begin{bmatrix} \frac{\tilde{\rho} e^{i\tilde{\psi}}}{\sqrt{1-\tilde{\rho}^2}} & \sqrt{1-\tilde{\rho}^2} \\ \sqrt{1-\tilde{\rho}^2} & -\tilde{\rho} e^{-i\tilde{\psi}} \end{bmatrix},$$

where  $0 \leq \tilde{\rho} \leq 1$  and  $0 \leq \tilde{\kappa}, \tilde{\psi} \leq 2\pi$ . The determinant of the matrix  $\mathbf{F}$  is

$$\det \mathbf{F} = -0.5 \det \mathbf{V} (1 - 2\tilde{\rho}^2 \sin^2 \tilde{\psi}) \|\mathbf{V}\|_F^2.$$

For a generic BIC, both  $\det \mathbf{V}$  and  $\|\mathbf{V}\|_F$  are nonzero. In addition, we show that  $(1 - 2\tilde{\rho}^2 \sin^2 \tilde{\psi}) = 0$  if and only if  $\tilde{\rho} \sin \tilde{\psi} = 0$  since  $\mathbf{S}^{1/2} \mathbf{S}^{1/2} = \mathbf{S}$ . Therefore, if nearly circular polarization cannot occur, we must have  $\det \mathbf{F} \neq 0$ . In this case, we can further show that  $\|\mathbf{F}^{-1} \mathbf{g}\|_2 < 1$ . Consequently, the trajectory  $(S_{d1}, S_{d2})$ ,  $\theta \in [-\pi, \pi)$  forms an ellipse with two revolutions around the origin. The revolution direction depends on the sign of  $\det \mathbf{F}$  (or  $\mathbf{S}$  and  $\mathbf{V}$ ).

#### S5. NUMERICAL METHODS

Figures 1 and 4 are calculated by Dirichlet-to-Neumann method introduced in Ref. [63]. Figures 2 and 3 are calculated by transverse impedance operator method developed in Ref. [64].